Chapter 3

The Seismic Wave Equation

Using the stress and strain theory developed in the previous chapter, we now construct and solve the seismic wave equation for elastic wave propagation in a uniform whole space. We will show that two types of solutions are possible, corresponding to compressional (P) and shear (S) waves, and we will derive the equations for their velocities that we presented in the last chapter. This will involve vector calculus and complex numbers; some of the mathematics is reviewed in Appendix 2. For simplicity, in this chapter we assume perfect elasticity with no energy loss in the seismic waves from any intrinsic attenuation.

3.1 Introduction: The Wave Equation

To motivate our discussion, consider the one-dimensional wave equation

$$\frac{\partial^2 u}{\partial t^2} = c^2 \frac{\partial^2 u}{\partial x^2} \tag{3.1}$$

and its general solution

$$u(x,t) = f(x \pm ct), \tag{3.2}$$

which represents waves of arbitrary shape propagating at velocity c in the positive and negative x directions. This is a very common equation in physics and can be used to describe, for example, the vibrations of a string or acoustic waves in a pipe. The velocity of the wave is determined by the physical properties of the material through which it propagates. In the case of a vibrating string, $c^2 = F/\rho$ where F is the string tension force and ρ is the density.

The wave equation is classified as a *hyperbolic equation* in the theory of linear partial differential equations. Hyperbolic equations are among the most challenging to solve because sharp features in their solutions will persist and can reflect off boundaries. Unlike, for example, the diffusion equation, solutions will be smooth only if the initial conditions are smooth. This complicates both analytical and numerical solution methods.

As we will see, the seismic wave equation is more complicated than equation (3.1) because it is three dimensional and the link between force and displacement

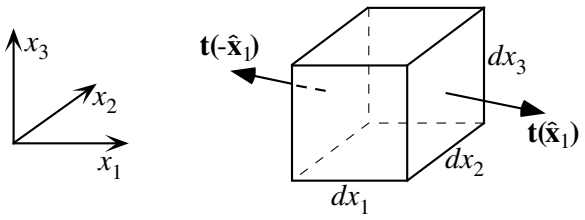

Figure 3.1: The force on the (x_2, x_3) face of an infinitesimal cube is given by $\mathbf{t}(\hat{\mathbf{x}}_1)\, dx_2\, dx_3$, the product of the traction vector and the surface area.

involves the full stress-strain relationship for an elastic solid. However, the P and S seismic wave solutions share many characteristics with the solutions to the 1-D wave equation. They involve pulses of arbitrary shape that travel at speeds determined by the elastic properties and density of the medium, and these pulses are often decomposed into harmonic wave solutions involving sine and cosine functions. Stein and Wysession (2003, section 2.2) provide a useful review of the 1-D wave equation as applied to a vibrating string, with analogies to seismic wave propagation in the Earth.

3.2 The Momentum Equation

In the previous chapter, the stress, strain, and displacement fields were considered in static equilibrium and unchanging with time. However, because seismic waves are time-dependent phenomena that involve velocities and accelerations, we need to account for the effect of momentum. We do this by applying Newton's law ($F = ma$ from your freshman physics class) to a continuous medium.

Consider the forces on an infinitesimal cube in a (x_1, x_2, x_3) coordinate system (Figure 3.1). The forces on each surface of the cube are given by the product of the traction vector and the surface area. For example, the force on the plane normal to x_1 is given by

$$\begin{aligned} \mathbf{F}(\hat{\mathbf{x}}_1) &= \mathbf{t}(\hat{\mathbf{x}}_1)\, dx_2\, dx_3 \\ &= \boldsymbol{\tau}\hat{\mathbf{x}}_1\, dx_2\, dx_3 \\ &= \begin{bmatrix} \tau_{11} \\ \tau_{21} \\ \tau_{31} \end{bmatrix} dx_2\, dx_3, \end{aligned} \tag{3.3}$$

where $\mathbf{F}$ is the force vector, $\mathbf{t}$ is the traction vector, and $\boldsymbol{\tau}$ is the stress tensor. In the case of a homogeneous stress field, there is no net force on the cube since the forces on opposing sides will cancel out, that is, $\mathbf{F}(-\hat{\mathbf{x}}_1) = -\mathbf{F}(\hat{\mathbf{x}}_1)$. Net force will only be exerted on the cube if spatial gradients are present in the stress field. In this case, the net force from the planes normal to x_1 is

$$\mathbf{F}(\hat{\mathbf{x}}_1) = \frac{\partial}{\partial x_1} \begin{bmatrix} \tau_{11} \\ \tau_{21} \\ \tau_{31} \end{bmatrix} dx_1\, dx_2\, dx_3, \tag{3.4}$$

and we can use index notation and the summation convention to express the total force from the stress field on all the faces of the cube as

$$\begin{aligned} F_i &= \sum_{j=1}^{3} \frac{\partial \tau_{ij}}{\partial x_j}\, dx_1\, dx_2\, dx_3 \\ &= \partial_j \tau_{ij}\, dx_1\, dx_2\, dx_3. \end{aligned} \tag{3.5}$$

The $d_j \tau_{ij}$ term is the divergence of the stress tensor (recall that summation convention means that this term is summed over $j = 1, 2, 3$). There may also exist a body force on the cube that acts in proportion to the volume of material, that is,

$$F_i^{\text{body}} = f_i\, dx_1\, dx_2\, dx_3. \tag{3.6}$$

The mass of our infinitesimal cube is given by

$$m = \rho\, dx_1\, dx_2\, dx_3, \tag{3.7}$$

where ρ is the density. The acceleration of the cube is given by the second time derivative of the displacement $\mathbf{u}$. Substituting (3.5)–(3.7) into $F = ma$ and canceling the common factor of $dx_1\, dx_2\, dx_3$, we obtain[1]

$$\rho \frac{\partial^2 u_i}{\partial t^2} = \partial_j \tau_{ij} + f_i. \tag{3.8}$$

This is the fundamental equation that underlies much of seismology. It is called the *momentum equation* or the *equation of motion* for a continuum. Each of the terms, u_i, τ_{ij} and f_i is a function of position $\mathbf{x}$ and time. The body force term $\mathbf{f}$ generally consists of a gravity term $\mathbf{f}_g$ and a source term $\mathbf{f}_s$. Gravity is an important factor at very low frequencies in normal mode seismology, but it can generally be neglected for body- and surface-wave calculations at typically observed wavelengths. We will consider the effects of the source term $\mathbf{f}_s$ later in this book (Chapter 9). In the absence of body forces, we have the *homogeneous equation of motion*

$$\rho \frac{\partial^2 u_i}{\partial t^2} = \partial_j \tau_{ij}, \tag{3.9}$$

which governs seismic wave propagation outside of seismic source regions. Generating solutions to (3.8) or (3.9) for realistic Earth models is an important part of seismology; such solutions provide the predicted ground motion at specific locations at some distance from the source and are commonly termed *synthetic seismograms*.

If, on the other hand, we assume that the acceleration term in (3.8) is zero, the result is the *static equilibrium equation*

$$\partial_j \tau_{ij} = -f_i. \tag{3.10}$$

[1] In expressing the acceleration term, we approximate the *total* derivatives of $\mathbf{u}$ with respect to time with the *partial* derivatives of $\mathbf{u}$ with respect to time. That is, we make the small-deformation approximation such that the terms in the total derivative containing the spatial derivatives of $\mathbf{u}$ can be ignored. This is generally assumed valid in seismology, but the spatial derivatives (advection terms) are very important in fluid mechanics.

in which the body forces are balanced by the divergence of the stress tensor. This equation is applicable to static deformation problems in geodesy, engineering and many other fields.

3.3 The Seismic Wave Equation

In order to solve (3.9) we require a relationship between stress and strain so that we can express $\boldsymbol{\tau}$ in terms of the displacement $\mathbf{u}$. Recall the linear, isotropic stress–strain relationship,

$$\tau_{ij} = \lambda \delta_{ij} e_{kk} + 2\mu e_{ij}, \tag{3.11}$$

where λ and μ are the Lamé parameters and the strain tensor is defined as

$$e_{ij} = \tfrac{1}{2}(\partial_i u_j + \partial_j u_i). \tag{3.12}$$

Substituting for e_{ij} in (3.11), we obtain

$$\tau_{ij} = \lambda \delta_{ij} \partial_k u_k + \mu(\partial_i u_j + \partial_j u_i). \tag{3.13}$$

Equations (3.9) and (3.13) provide a coupled set of equations for the displacement and stress. These equations are sometimes used directly at this point to model wave propagation in computer calculations by applying finite-difference techniques. In these methods, the stresses and displacements are computed at a series of grid points in the model, and the spatial and temporal derivatives are approximated through numerical differencing. The great advantage of finite-difference schemes is their relative simplicity and ability to handle Earth models of arbitrary complexity. However, they are extremely computationally intensive and do not necessarily provide physical insight regarding the behavior of the different wave types.

In the equations that follow, we will switch back and forth between vector notation and index notation. A brief review of vector calculus is given in Appendix B. If we substitute (3.13) into (3.9), we obtain

$$\begin{aligned} \rho \frac{\partial^2 u_i}{\partial t^2} &= \partial_j[\lambda \delta_{ij} \partial_k u_k + \mu(\partial_i u_j + \partial_j u_i)] \\ &= \partial_i \lambda \partial_k u_k + \lambda \partial_i \partial_k u_k + \partial_j \mu(\partial_i u_j + \partial_j u_i) + \mu \partial_j \partial_i u_j + \mu \partial_j \partial_j u_i \\ &= \partial_i \lambda \partial_k u_k + \partial_j \mu(\partial_i u_j + \partial_j u_i) + \lambda \partial_i \partial_k u_k + \mu \partial_i \partial_j u_j + \mu \partial_j \partial_j u_i. \end{aligned} \tag{3.14}$$

Defining $\ddot{\mathbf{u}} = \partial^2 \mathbf{u}/\partial t^2$, we can write this in vector notation as

$$\rho \ddot{\mathbf{u}} = \nabla \lambda (\nabla \cdot \mathbf{u}) + \nabla \mu \cdot [\nabla \mathbf{u} + (\nabla \mathbf{u})^T] + (\lambda + \mu) \nabla \nabla \cdot \mathbf{u} + \mu \nabla^2 \mathbf{u}. \tag{3.15}$$

We now use the vector identity

$$\nabla \times \nabla \times \mathbf{u} = \nabla \nabla \cdot \mathbf{u} - \nabla^2 \mathbf{u} \tag{3.16}$$

to change this to a more convenient form. We have

$$\nabla^2 \mathbf{u} = \nabla \nabla \cdot \mathbf{u} - \nabla \times \nabla \times \mathbf{u}. \tag{3.17}$$

Substituting this into (3.15), we obtain

$$\rho\ddot{\mathbf{u}} = \nabla\lambda(\nabla\cdot\mathbf{u}) + \nabla\mu\cdot[\nabla\mathbf{u} + (\nabla\mathbf{u})^T] + (\lambda+2\mu)\nabla\nabla\cdot\mathbf{u} - \mu\nabla\times\nabla\times\mathbf{u}. \quad (3.18)$$

This is one form of the *seismic wave equation*. The first two terms on the right-hand side (r.h.s.) involve gradients in the Lamé parameters themselves and are nonzero whenever the material is inhomogeneous (i.e., contains velocity gradients). Most non trivial Earth models for which we might wish to compute synthetic seismograms contain such gradients. However, including these factors makes the equations very complicated and difficult to solve efficiently. Thus, most practical synthetic seismogram methods ignore these terms, using one of two different approaches.

First, if velocity is only a function of depth, then the material can be modeled as a series of homogeneous layers. Within each layer, there are no gradients in the Lamé parameters and so these terms go to zero. The different solutions within each layer are linked by calculating the reflection and transmission coefficients for waves at both sides of the interface separating the layers. The effects of a continuous velocity gradient can be simulated by considering a "staircase" model with many thin layers. As the number of layers increases, these results can be shown to converge to the continuous gradient case (more layers are needed at higher frequencies). This approach forms the basis for many techniques for computing predicted seismic motions from one-dimensional Earth models; we will term these *homogeneous-layer methods*. They are particularly useful for studying surface waves and low- to medium-frequency body waves. However, at high frequencies they become relatively inefficient because large numbers of layers are necessary for accurate modeling.

Second, it can be shown that the strength of these gradient terms varies as $1/\omega$, where ω is frequency, and thus at high frequencies these terms will tend to zero. This approximation is made in most *ray-theoretical methods*, in which it is assumed that the frequencies are sufficiently high that the $1/\omega$ terms are unimportant. However, note that at any given frequency this approximation will break down if the velocity gradients in the material become steep enough. At velocity discontinuities between regions of shallow gradients, the approximation cannot be used directly, but the solutions above and below the discontinuities can be patched together through the use of reflection and transmission coefficients. The distinction between the homogeneous-layer and ray-theoretical approaches is often important and will be emphasized later in this book.

If we ignore the gradient terms, the momentum equation for homogeneous media becomes

$$\rho\ddot{\mathbf{u}} = (\lambda+2\mu)\nabla\nabla\cdot\mathbf{u} - \mu\nabla\times\nabla\times\mathbf{u}. \quad (3.19)$$

This is a standard form for the seismic wave equation in homogeneous media and forms the basis for most body wave synthetic seismogram methods. However, it is important to remember that it is an approximate expression, which has neglected the gravity and velocity gradient terms and has assumed a linear, isotropic Earth model.

We can separate this equation into solutions for P-waves and S-waves by taking the divergence and curl, respectively. Taking the divergence of (3.19) and using the

vector identity $\nabla \cdot (\nabla \times \mathbf{\Psi}) = 0$, we obtain:

$$\frac{\partial^2(\nabla \cdot \mathbf{u})}{\partial t^2} = \frac{\lambda + 2\mu}{\rho} \nabla^2(\nabla \cdot \mathbf{u}) \tag{3.20}$$

or

$$\nabla^2(\nabla \cdot \mathbf{u}) - \frac{1}{\alpha^2} \frac{\partial^2(\nabla \cdot \mathbf{u})}{\partial t^2} = 0, \tag{3.21}$$

where the P-wave velocity, α, is given by

$$\alpha^2 = \frac{\lambda + 2\mu}{\rho}. \tag{3.22}$$

Taking the curl of (3.19) and using the vector identity $\nabla \times (\nabla \phi) = 0$, we obtain:

$$\frac{\partial^2(\nabla \times \mathbf{u})}{\partial t^2} = -\frac{\mu}{\rho} \nabla \times \nabla \times (\nabla \times \mathbf{u}). \tag{3.23}$$

Using the vector identity (3.16) and $\nabla \cdot (\nabla \times \mathbf{u}) = 0$, this becomes

$$\frac{\partial^2(\nabla \times \mathbf{u})}{\partial t^2} = \frac{\mu}{\rho} \nabla^2(\nabla \times \mathbf{u}) \tag{3.24}$$

or

$$\nabla^2(\nabla \times \mathbf{u}) - \frac{1}{\beta^2} \frac{\partial^2(\nabla \times \mathbf{u})}{\partial t^2} = 0, \tag{3.25}$$

where the S-wave velocity, β, is given by

$$\beta^2 = \frac{\mu}{\rho}. \tag{3.26}$$

We can use (3.22) and (3.26) to rewrite the elastic wave equation (3.18) directly in terms of the P and S velocities:

$$\ddot{\mathbf{u}} = \alpha^2 \nabla \nabla \cdot \mathbf{u} - \beta^2 \nabla \times \nabla \times \mathbf{u}. \tag{3.27}$$

3.3.1 Potentials

The displacement $\mathbf{u}$ is often expressed in terms of the P-wave scalar potential ϕ and S-wave vector potential $\mathbf{\Psi}$, using the Helmholtz decomposition theorem (e.g., p. 67–69 of Aki and Richards, 2002), i.e.,

$$\mathbf{u} = \nabla \phi + \nabla \times \mathbf{\Psi}, \quad \nabla \cdot \mathbf{\Psi} = 0. \tag{3.28}$$

We then have

$$\nabla \cdot \mathbf{u} = \nabla^2 \phi \tag{3.29}$$

and

$$\begin{aligned} \nabla \times \mathbf{u} &= \nabla \times \nabla \times \mathbf{\Psi} \\ &= \nabla \nabla \cdot \mathbf{\Psi} - \nabla^2 \mathbf{\Psi} \quad \text{(from 3.16)} \\ &= -\nabla^2 \mathbf{\Psi} \quad \text{(since } \nabla \cdot \mathbf{\Psi} = 0\text{)}. \end{aligned} \tag{3.30}$$

Table 3.1: Harmonic wave parameters.

Angular frequency	ω	time^{-1}	$\omega = 2\pi f = \frac{2\pi}{T} = ck$
Frequency	f	time^{-1}	$f = \frac{\omega}{2\pi} = \frac{1}{T} = \frac{c}{\Lambda}$
Period	T	time	$\mathrm{T} = \frac{1}{f} = \frac{2\pi}{\omega} = \frac{\Lambda}{c}$
Velocity	c	distance time^{-1}	$c = \frac{\Lambda}{T} = f\Lambda = \frac{\omega}{k}$
Wavelength	Λ	distance	$\Lambda = \frac{c}{f} = cT = \frac{2\pi}{k}$
Wavenumber	k	distance^{-1}	$k = \frac{\omega}{c} = \frac{2\pi}{\Lambda} = \frac{2\pi f}{c} = \frac{2\pi}{cT}$

Motivated by (3.21) and (3.25), we require that these potentials also satisfy

$$\nabla^2\phi - \frac{1}{\alpha^2}\frac{\partial^2\phi}{\partial t^2} = 0, \tag{3.31}$$

$$\nabla^2\mathbf{\Psi} - \frac{1}{\beta^2}\frac{\partial^2\mathbf{\Psi}}{\partial t^2} = 0. \tag{3.32}$$

After solving these equations for ϕ and $\mathbf{\Psi}$, the P-wave displacement is given by the gradient of ϕ and the S-wave displacement is given by the curl of $\mathbf{\Psi}$, following (3.28).

3.4 Plane Waves

At this point it is helpful to introduce the concept of a *plane wave*. This is a solution to the wave equation in which the displacement varies only in the direction of wave propagation and is constant in the directions orthogonal to the propagation direction. For example, for a plane wave traveling along the x axis, the displacement may be expressed as

$$\mathbf{u}(x,t) = \mathbf{f}(t \pm x/c), \tag{3.33}$$

where c is the velocity of the wave, $\mathbf{f}$ is any arbitrary function (a vector function is required to express the polarization of the wave), and the waves are propagating in either the $+x$ or $-x$ direction. The displacement does not vary with y or z; the wave extends to infinity in these directions. If $\mathbf{f}(t)$ is a discrete pulse, then u assumes the form of a displacement pulse traveling as a planar wavefront. More generally, displacement at position vector $\mathbf{x}$ for a plane wave propagating in the unit direction $\hat{\mathbf{s}}$ may be expressed as

$$\mathbf{u}(\mathbf{x},t) = \mathbf{f}(t - \hat{\mathbf{s}}\cdot\mathbf{x}/c) \tag{3.34}$$

$$= \mathbf{f}(t - \mathbf{s}\cdot\mathbf{x}), \tag{3.35}$$

where $\mathbf{s} = \hat{\mathbf{s}}/c$ is the *slowness vector*, whose magnitude is the reciprocal of the velocity.

Since seismic energy is usually radiated from localized sources, seismic wavefronts are always curved to some extent; however, at sufficiently large distances

from the source the wavefront becomes flat enough that a plane wave approximation becomes locally valid. Furthermore, many techniques for solving the seismic wave equation involve expressing the complete solution as a sum of plane waves of differing propagation angles. Often the time dependence is also removed from the equations by transforming into the frequency domain. In this case the displacement for a particular angular frequency ω may be expressed as

$$\begin{aligned} \mathbf{u}(\mathbf{x},t) &= \mathbf{A}(\omega)e^{-i\omega(t-\mathbf{s}\cdot\mathbf{x})} && (3.36)\\ &= \mathbf{A}(\omega)e^{-i(\omega t-\mathbf{k}\cdot\mathbf{x})}, && (3.37)\end{aligned}$$

where $\mathbf{k} = \omega\mathbf{s} = (\omega/c)\hat{\mathbf{s}}$ is termed the *wavenumber vector*. We will use complex numbers to represent harmonic waves throughout this book; details of how this works are reviewed in Appendix B. This may be termed a *monochromatic* plane wave; it is also sometimes called the *harmonic* or *steady-state* plane wave solution. Other parameters used to describe such a wave are the wavenumber $k = |\mathbf{k}| = \omega/c$, the frequency $f = \omega/(2\pi)$, the period $T = 1/f$, and the wavelength $\Lambda = cT$. Equations relating the various harmonic wave parameters are summarized in Table 3.1.

3.4.1 Example: Harmonic plane wave equation

What is the equation for the displacement of a 1 Hz P-wave propagating in the $+x$ direction at 6 km/s? In this case $\omega = 2\pi f$, where $f = 1$ Hz, and thus $\omega = 2\pi$. The slowness vector is in the direction of the x-axis and thus $\hat{\mathbf{s}} = \hat{\mathbf{x}} = (1,0,0)$ and $\mathbf{s} = (1/c,0,0) = (1/6,0,0)$ s/km. We can thus express (3.36) as

$$\mathbf{u}(\mathbf{x},t) = \mathbf{u}(x,t) = \mathbf{A}e^{-2i\pi(t-x/6)}$$

where t is in s and x is in km. As we will see in the next section, P waves are polarized in the direction of wave propagation, so $\mathbf{u} = (u_x,0,0)$ and we can express this more simply as

$$u_x(x,t) = Ae^{-2i\pi(t-x/6)}$$

In general, the coefficient A is complex to permit any desired phase at $x = 0$. As described in Appendix B, the real part must be taken for this equation to have a physical meaning. An alternative form is

$$u_x(x,t) = a\cos\left[2\pi(t-x/6)-\phi\right]$$

where a is the amplitude and ϕ is the phase at $x = 0$ (see Figure B.3).

3.5 Polarizations of P and S Waves

Consider plane P-waves propagating in the x direction. From (3.31) we have

$$\alpha^2\partial_{xx}\phi = \partial_{tt}\phi. \qquad (3.38)$$

A general solution to (3.38) can be written as

$$\phi = \phi_0(t \pm x/\alpha), \tag{3.39}$$

where a minus sign corresponds to propagation in the $+x$ direction and a plus sign denotes propagation in the $-x$ direction. Because $\mathbf{u} = \nabla\phi$, we have

$$\begin{aligned} u_x &= \partial_x\phi, \\ u_y &= 0, \\ u_z &= 0. \end{aligned} \tag{3.40}$$

Note that for a plane wave propagating in the x direction there is no change in the y and z directions, and so the spatial derivatives ∂_y and ∂_z are zero. For P-waves, the only displacement occurs in the direction of propagation along the x axis. Such wave motion is termed "longitudinal." Also, because $\nabla \times \nabla\phi = 0$, the motion is curl-free or "irrotational." Since P-waves introduce volume changes in the material ($\nabla \cdot \mathbf{u} \neq 0$), they can also be termed "compressional" or "dilatational." However, note that P-waves involve shearing as well as compression; this is why the P velocity is sensitive to both the bulk and shear moduli. Particle motion for a harmonic P-wave is shown in Figure 3.2.

Now consider a plane S-wave propagating in the positive x direction. The vector potential becomes

$$\mathbf{\Psi} = \Psi_x(t - x/\beta)\hat{\mathbf{x}} + \Psi_y(t - x/\beta)\hat{\mathbf{y}} + \Psi_z(t - x/\beta)\hat{\mathbf{z}}. \tag{3.41}$$

The displacement is

$$\begin{aligned} u_x = (\nabla \times \mathbf{\Psi})_x &= \partial_y\Psi_z - \partial_z\Psi_y = 0, \\ u_y = (\nabla \times \mathbf{\Psi})_y &= \partial_z\Psi_x - \partial_x\Psi_z = -\partial_x\Psi_z, \\ u_z = (\nabla \times \mathbf{\Psi})_z &= \partial_x\Psi_y - \partial_y\Psi_x = \partial_x\Psi_y, \end{aligned} \tag{3.42}$$

where again we have used $\partial_y = \partial_z = 0$, thus giving

$$\mathbf{u} = -\partial_x\Psi_z\hat{\mathbf{y}} + \partial_x\Psi_y\hat{\mathbf{z}}. \tag{3.43}$$

The motion is in the y and z directions, perpendicular to the propagation direction. S-wave particle motion is often divided into two components: the motion within a vertical plane through the propagation vector (SV-waves) and the horizontal motion in the direction perpendicular to this plane (SH-waves). Because $\nabla \cdot \mathbf{u} = \nabla \cdot (\nabla \times \mathbf{\Psi}) = 0$, the motion is pure shear without any volume change (hence the name shear waves). Particle motion for a harmonic shear wave polarized in the vertical direction (SV-wave) is illustrated in Figure 3.2.

3.6 Spherical Waves

Another solution to the scalar wave equation (3.31) for the P-wave potential ϕ is possible if we assume spherical symmetry. In spherical coordinates, the Laplacian operator is

$$\nabla^2\phi(r) = \frac{1}{r^2}\frac{\partial}{\partial r}\left[r^2\frac{\partial\phi}{\partial r}\right], \tag{3.44}$$

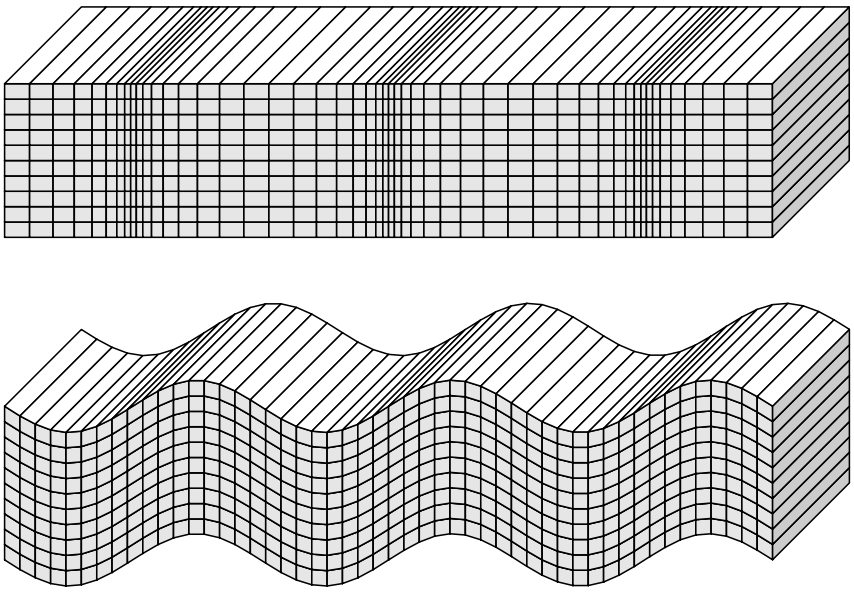

Figure 3.2: Displacements occurring from a harmonic plane P-wave (top) and S-wave (bottom) traveling horizontally across the page. S-wave propagation is pure shear with no volume change, whereas P-waves involve both a volume change and shearing (change in shape) in the material. Strains are highly exaggerated compared to actual seismic strains in the Earth.

where we have dropped the angular derivatives because of the spherical symmetry. Using this expression in (3.31), we have

$$\frac{1}{r^2}\frac{\partial}{\partial r}\left[r^2\frac{\partial \phi}{\partial r}\right] - \frac{1}{\alpha^2}\frac{\partial^2 \phi}{\partial t^2} = 0. \tag{3.45}$$

Solutions to this equation outside the point $r = 0$ may be expressed as

$$\phi(r,t) = \frac{f(t \pm r/\alpha)}{r}. \tag{3.46}$$

Note that this is identical to the plane wave equation (3.33), except for the factor of $1/r$. Inward and outward propagating waves are specified by the $+$ and $-$ signs respectively. Since this expression is usually used to model waves radiating away from a point source, the inward propagating solution is normally ignored. In this case the $1/r$ term represents a decay in the wave amplitude with range, a geometrical spreading factor that we will explore further in Chapter 6.

Equation (3.46) is not a valid solution to (3.45) at $r = 0$. However, it can be shown (e.g., Aki and Richards, 2002, Section 4.1) that (3.46) is the solution to the inhomogeneous wave equation

$$\nabla^2\phi(r) - \frac{1}{\alpha^2}\frac{\partial^2 \phi}{\partial t^2} = -4\pi\delta(r)f(t), \tag{3.47}$$

where the delta function $\delta(r)$ is zero everywhere except $r = 0$ and has a volume integral of one. The factor $4\pi\delta(r)f(t)$ represents the source–time function at the

origin. We will return to this equation when we discuss seismic source theory in Chapter 9.

3.7 Methods for Computing Synthetic Seismograms†

A large part of seismology involves devising and implementing techniques for computing synthetic seismograms for realistic Earth models. In general, our goal is to calculate what would be recorded by a seismograph at a specified receiver location, given an exact specification of the seismic source and the Earth model through which the seismic waves propagate. This is a well-defined forward problem that, in principle, can be solved exactly. However, errors in the synthetic seismograms often occur in practical applications. These inaccuracies can be be separated into two parts:

1. Inaccuracies arising from approximations in the theory used to compute the synthetic seismograms. Examples of this would include many applications of ray theory which do not properly account for head waves, diffracted waves, or the coupling between different waves types at long periods. Another computational error is the grid dispersion that occurs in most finite difference schemes.

2. Errors caused by using a simplified Earth or source model. In this case the synthetic seismogram may be exact for the simplied model, but the model is an inadequate representation of the real problem. These simplifications might be necessary in order to apply a particular numerical technique, or might result from ignorance of many of the details of the model. Examples would include the use of 1-D models that do not fully account for 3-D structure, the assumption of a point source rather than a finite rupture, and neglecting the effects of attenuation or anisotropy in the calculations.

The first category of errors may be addressed by applying a more exact algorithm, although in practice limits on computing resources may prevent achieving the desired accuracy in the case of complicated models. The second category is more serious because often one simply does not know the properties of the Earth well enough to be able to model every wiggle in the observed seismograms. This is particularly true at high frequencies (0.5 Hz and above). For teleseismic arrivals, long-period body waves (15–50 s period) and surface waves (40–300 s period) can usually be fit well with current Earth models, whereas the coda of high-frequency body wave arrivals can only be modeled statistically (fitting the envelope function but not the individual wiggles).

Because of the linearity of the problem and the superposition principle (in which distributed sources can be described as the sum of multiple point sources), there is no great difficulty in modeling even very complicated sources (inverting for these sources, is, of course, far more difficult, but here we are only concerned with the forward problem). If the source can be exactly specified, then computing synthetics for a distributed source is only slightly more complicated than for a simple point

source. By far the most difficult part in computing synthetic seismgrams is solving for the propogation effects through realistic velocity structures. Only for a few grossly simplified models (e.g., whole space or half-spaces) are analytical solutions possible.

The part of the solution that connects the force distribution at the source with the displacements at the receiver is termed the elastodynamic Green's function, and will be discussed in greater detail in Chapter 9. Computation of the Green's function is the key part of the synthetic seismogram calculation because this function must take into account all of the elastic properties of the material and the appropriate boundary conditions.

There are a large number of different methods for computing synthetic seismograms. Most of these fall into the following categories:

1. Finite-difference and finite-element methods that use computer power to solve the wave equation over a discrete set of grid points or model elements. These have the great advantage of being able to handle models of arbitrary complexity. Their computational cost grows with the number of required grid points; more points are required for 3-D models (vs. 2-D) and for higher frequencies. These methods are discussed in more detail in the next section.

2. Ray-theoretical methods in which ray geometries are explicitly specified and ray paths are computed. These methods include simple (or geometrical) ray theory, WKBJ, and so-called "generalized" ray theory. They are most useful at high frequencies for which the ray-theoretical approximation is most accurate. They are most simply applied to 1-D Earth models but can be generalized to 3-D models.

3. Homogeneous layer methods in which the model consists of a series of horizontal layers with constant properties within each layer. Matrix methods are then used to connect the solutions between layers. Examples of this approach include "reflectivity" and "wavenumber integration." These methods yield an exact solution but can become moderately computationally intensive at high frequencies because a large number of layers are required to accurately simulate continuous velocity gradients. Unlike finite-difference and ray-theoretical methods, homogeneous-layer techniques are restricted to 1-D Earth models. However, spherically symmetric models can be computed using the Flat Earth Transformation.

4. Normal mode summation methods in which the standing waves (eigenvectors) of the spherical Earth are computed and then summed to generate synthetic seismograms. This is the most natural and complete way to compute synthetic seismograms for the spherical Earth, but is computationally intensive at high frequencies. Generalization to 3-D Earth models requires including coupling between modes; this is generally done using asymptotic approximations and greatly increases the complexity of the algorithm.

There is no single "best" way to compute synthetic seismograms as each method has its own advantages and disadvantages. The method of choice will depend upon

the particular problem to be addressed and the available computer power; thus it is useful to be aware of the full repertoire of techniques. This book will cover only how relatively simple ray-theoretical synthetic seismograms can be computed for 1-D Earth models. For details regarding ray-theoretical and homogeneous-layer methods, see Kennett (2001) and Chapman (2004). For normal mode methods, see Dahlen and Tromp (1998).

3.8 The Future of Seismology?†

Increasing computer capabilities now make possible ambitious numerical simulations of seismic wave propagation that were impractical only a few years ago and this trend is likely to continue for many decades. These calculations involve finite-difference or finite-element methods that approximate the continuum of elastic properties with a large number of discrete values or model elements and solve the wave equation numerically over a series of discrete time steps. They provide a complete image of the wavefield at each point in the model for every time step, as illustrated in Figure 3.3, which shows a snapshot at 10 minutes of the SH wavefield in the mantle for a source at 500 km (Thorne et al., 2007). Finite difference methods specify the model at a series of grid points and approximate the spatial and temporal derivatives by using the model values at nearby grid points. Finite element methods divide the model into a series of volume elements with specified properties and match the appropriate boundary conditions among adjacent elements. Historically, because of their simplicity, finite-difference methods have been used in seismology more often than finite elements. However, finite-difference algorithms can have difficulty correctly handling boundary conditions at sharp interfaces, including the irregular topography at the Earth's surface, for which finite-element schemes are more naturally suited.

Discrete modeling approaches can accurately compute seismograms for complicated 3-D models of Earth structure, provided the gridding or meshing scheme has sufficient resolution. Complicated analytical techniques are not required, although the speed of the algorithm depends upon the skill of the computer programmer in developing efficient code. Typically, a certain number of grid points or model elements are required per seismic wavelength for accurate results, with the exact number depending upon the specific algorithm. In three dimensions, the number of grid points grows inversely as the cube of the grid spacing and number of required time steps normally also increases. Because of this, computational requirements increase rapidly with decreasing seismic wavelength, with the most challenging calculations being at high frequencies and the greatest required grid densities occurring in the slowest parts of the model.

Finite difference methods vary depending upon how the temporal and spatial derivatives in these equations are calculated. Simple first-order differencing schemes for the spatial derivatives are fast and easy to program, but require more grid points per wavelength to achieve accuracy comparable to higher-order differencing schemes. Many finite-difference programs use the staggered grid approach in which the velocities and stresses are computed at different grid points.

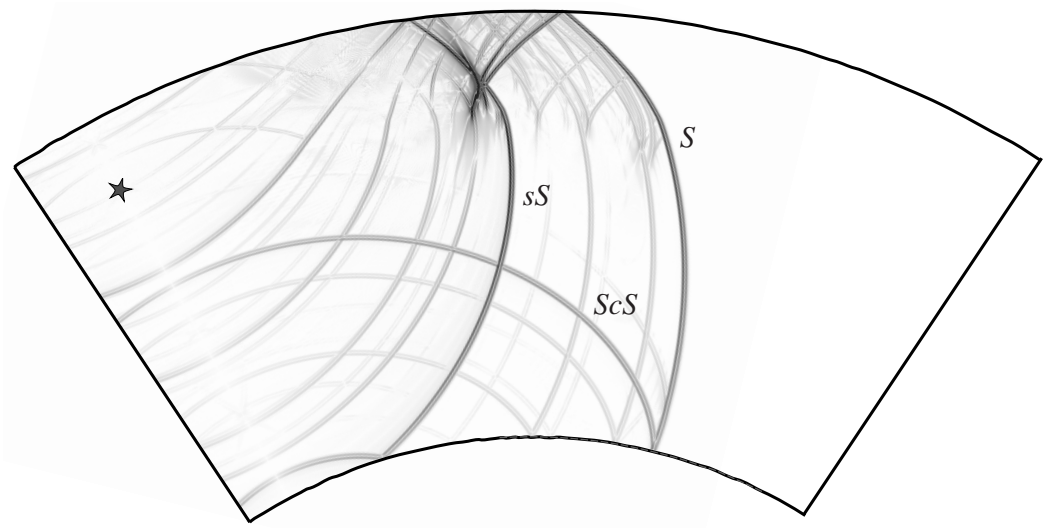

Figure 3.3: The SH-velocity wavefield in the mantle after 10 minutes for a source at 500 km depth (star), adapted from a figure in Thorne et al. (2007). This axi-symmetric 2-D finite-difference calculation used the PREM velocity model. The major seismic phases are labeled (see Chapter 4); the lower amplitude phases are mainly reflections off upper-mantle discontinuities and an assumed discontinuity 264 km above the core-mantle boundary.

A few general points to keep in mind:

1. Finite-difference programs run most efficiently if their arrays fit into memory and thus machines with large memories are desirable. Higher-order finite-difference schemes generally have an advantage because fewer grid points per wavelength are required for accurate results, thus reducing the size of the arrays.

2. Simple first-order differencing schemes require more grid points per wavelength than higher-order schemes. A commonly used "rule of thumb" is that first-order differencing algorithms require about 20 grid points per wavelength, but even this is not sufficient if the calculation is performed for a large model that spans many wavelengths. So called *psuedo-spectral* methods are equivalent to very high order differencing methods and in principle require the smallest number of grid points per wavelength (approaching 2 in certain idealized situations). However, models with sharp velocity discontinuities often require more grid points, so much of the advantage of the spectral methods is lost in this case.

3. An important aspect of finite-difference and finite-element methods is devising absorbing boundary conditions to prevent annoying reflections from the edges of the model. This is a nontrivial problem and many papers have been written discussing various techniques. Many of these methods work adequately for waves hitting the boundaries at near normal incidence, but have problems for grazing incidence angles.

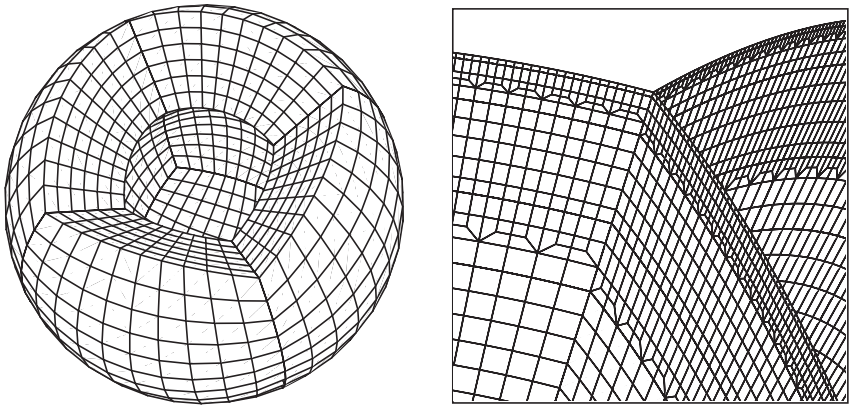

Figure 3.4: The meshing scheme used by the Komatitsch et al. (2002, 2005) implementation of the spectral element method. The spherical Earth is decomposed into six "cubical" blocks. The right plot shows how the blocks join and how the number of elements increases near the surface.

Finite-element programs often have advantages over finite differences in applying boundary conditions. Currently the most developed finite-element program in global seismology is the implementation of the spectral-element method by Komatitsch, Tromp and coworkers (e.g., Komatitsch et al., 2002, 2005), which explicitly includes the free-surface and fluid/solid boundary conditions at the core-mantle and inner-core boundaries. This program is designed to run in parallel on large high-performance computing clusters. It uses a variable size meshing scheme for the entire Earth that maintains a relatively constant number of grid points per wavelength (see Figure 3.4). The method includes the effects of general anisotropy, anelasticity (attenuation), surface topography, ellipticity, rotation, and self-gravitation. As implemented, the method requires an average of 5 grid points per wavelength for many applications. The algorithm has been validated through comparisons with synthetics computed using normal mode summation.

Numbers cited by Komatitsch et al. (2005) for calculations on the Earth Simulator at the Japan Agency for Marine Earth Science and Technology (JAMSTEC) provide some perspective on the computational requirements. Using 48 nodes (with 64 gigaflops and 16 gigabytes of memory per node), a global simulation can model wave periods down to 9 s in about 10 hours of computer time. Shorter periods can be reached in the same time if more nodes are used. This calculation provides synthetic seismograms from a single earthquake to any number of desired receivers. The Earth model itself can be arbitrarily complicated with calculations for general 3-D velocity and density variations taking no longer than those for 1-D reference models.

Large-scale numerical simulations are also important for modeling strong ground motions in and around sedimentary basins from large earthquakes and a number of groups are now performing these calculations (e.g., Akcelik et al., 2003; Olsen et al., 2006). A challenging aspect of these problems is the very slow shear velocities observed in shallow sedimentary layers. For example, in the Los Angeles basin the

average shear velocity approaches 200 m/s at the surface (e.g., Magistrale et al., 2000). These calculations are valuable because they show how focusing effects from rupture directivity and basin geometry can lead to large variations in expected wave amplitudes.

As computer speed and memory size increases, these numerical methods will become practical even on desktop machines and eventually it will be possible to routinely compute broadband synthetics for general 3-D Earth models. In time, these computer-intensive algorithms will probably replace many of the alternative synthetic seismogram methods. However there will still be a need for the techniques of classical seismology, such as ray theory and surface wave dispersion analysis, in order to understand and interpret the results that the computers provide. Ultimately the challenge will be to devise new methods of data analysis and inversion that will fully exploit the computational capabilities that are rapidly coming to the field.

3.9 Equations for 2-D Isotropic Finite Differences†

As an example of a discrete modeling method, this section presents equations for simple isotropic 1-D and 2-D finite differences. Much of this material is adapted from section 13.6 of the 2nd volume of the first edition of Aki and Richards (1980). We begin with the momentum equation:

$$\rho \frac{\partial^2 \mathbf{u}}{\partial t^2} = \nabla \cdot \boldsymbol{\tau} \tag{3.48}$$

Now let $\mathbf{u} = (u_x, u_y, u_z) = (u, v, w)$ and recall that $(\nabla \cdot \boldsymbol{\tau})_i = \partial_j \tau_{ij}$. For the two-dimensional case of SH-waves propagating in the x-z plane, displacement only occurs in the y-direction (i.e. $\mathbf{u} = (0, v, 0)$) and we can write:

$$\rho \frac{\partial^2 v}{\partial t^2} = \partial_j \tau_{yj} = \frac{\partial \tau_{yx}}{\partial x} + \frac{\partial \tau_{yz}}{\partial z} \tag{3.49}$$

Note that $\frac{\partial}{\partial y} = 0$ for the two-dimensional problem. Now recall (3.13) which relates stress to displacement for isotropic media:

$$\tau_{ij} = \lambda \delta_{ij} \partial_k u_k + \mu(\partial_i u_j + \partial_j u_i) \tag{3.50}$$

Using this equation we can obtain expressions for τ_{yx} and τ_{yz}:

$$\begin{aligned} \tau_{yx} &= \mu \tfrac{\partial v}{\partial x} \\ \tau_{yz} &= \mu \tfrac{\partial v}{\partial z} \end{aligned} \tag{3.51}$$

Substituting into (3.49), we obtain:

$$\rho \frac{\partial^2 v}{\partial t^2} = \frac{\partial}{\partial x}\left[\mu \frac{\partial v}{\partial x}\right] + \frac{\partial}{\partial z}\left[\mu \frac{\partial v}{\partial z}\right] \tag{3.52}$$

Note that for one-dimensional wave propagation in the x-direction $\frac{\partial}{\partial z} = 0$ and the SH equation reduces to:

$$\rho(x) \frac{\partial^2 v}{\partial t^2} = \frac{\partial}{\partial x}\left[\mu(x) \frac{\partial v}{\partial x}\right] \tag{3.53}$$

This is equivalent to equation (13.129) in Aki and Richards (1980). A similar equation exists for one-dimensional P-wave propagation if the $\mu(x)$ is replaced with $\lambda(x) + 2\mu(x)$ and the displacements in the y-direction (v) are replaced with displacements in the x-direction (u).

We can avoid the double time derivative and the space derivatives of μ if we use the particle velocity $\dot{v}$ and stress $\tau = \mu \partial v/\partial x$ as variables. We then have the simultaneous equations:

$$\begin{aligned} \frac{\partial \dot{v}}{\partial t} &= \frac{1}{\rho(x)} \frac{\partial \tau}{\partial x} \\ \frac{\partial \tau}{\partial t} &= \mu(x) \frac{\partial \dot{v}}{\partial x} \end{aligned} \tag{3.54}$$

A solution to these equations can be obtained directly using finite-difference approximations for the derivatives. In order to design a stable finite-difference algorithm for the wave equation, it is important to use *centered* finite-difference operators. To see this, consider the Taylor series expansion of a function $\phi(x)$

$$\phi(x+\Delta x) = \phi(x) + \frac{\partial \phi}{\partial x}\Delta x + \frac{1}{2}\frac{\partial^2 \phi}{\partial x^2}(\Delta x)^2 + \frac{1}{6}\frac{\partial^3 \phi}{\partial x^3}(\Delta x)^3 + \text{higher order terms} \tag{3.55}$$

If we solve this equation for $\partial\phi/\partial x$, we obtain

$$\frac{\partial \phi}{\partial x} = \frac{1}{\Delta x}\Big[\phi(x+\Delta x) - \phi(x)\Big] - \frac{1}{2}\frac{\partial^2 \phi}{\partial x^2}\Delta x - \frac{1}{6}\frac{\partial^3 \phi}{\partial x^3}(\Delta x)^2 - \ldots \tag{3.56}$$

and we see that the simple approximation

$$\frac{\partial \phi}{\partial x} \approx \frac{1}{\Delta x}\Big[\phi(x+\Delta x) - \phi(x)\Big] \tag{3.57}$$

will have a leading truncation error proportional to Δx. To obtain a better approximation, consider the expansion for $\phi(x - \Delta x)$

$$\phi(x-\Delta x) = \phi(x) - \frac{\partial \phi}{\partial x}\Delta x + \frac{1}{2}\frac{\partial^2 \phi}{\partial x^2}(\Delta x)^2 - \frac{1}{6}\frac{\partial^3 \phi}{\partial x^3}(\Delta x)^3 + \text{higher order terms} \tag{3.58}$$

Solving for $\partial\phi/\partial x$, we obtain

$$\frac{\partial \phi}{\partial x} = \frac{1}{\Delta x}\Big[\phi(x) - \phi(x-\Delta x)\Big] + \frac{1}{2}\frac{\partial^2 \phi}{\partial x^2}\Delta x - \frac{1}{6}\frac{\partial^3 \phi}{\partial x^3}(\Delta x)^2 - \ldots \tag{3.59}$$

Averaging (3.56) and (3.59), we obtain

$$\frac{\partial \phi}{\partial x} = \frac{1}{2\Delta x}\Big[\phi(x+\Delta x) - \phi(x-\Delta x)\Big] - \frac{1}{3}\frac{\partial^3 \phi}{\partial x^3}(\Delta x)^2 - \ldots \tag{3.60}$$

and we see that the central difference formula

$$\frac{\partial \phi}{\partial x} = \frac{1}{2\Delta x}\Big[\phi(x+\Delta x) - \phi(x-\Delta x)\Big] \tag{3.61}$$

has an error of order $(\Delta x)^2$. For small values of Δx, these errors will be much smaller than those obtained using (3.57). Similarly, the second derivative of ϕ can be computed by summing (3.55) and (3.58) to obtain

$$\frac{\partial^2 \phi}{\partial x^2} = \frac{1}{(\Delta x)^2}\Big[\phi(x + \Delta x) - 2\phi(x) + \phi(x - \Delta x)\Big] \tag{3.62}$$

which also has error of order $(\Delta x)^2$.

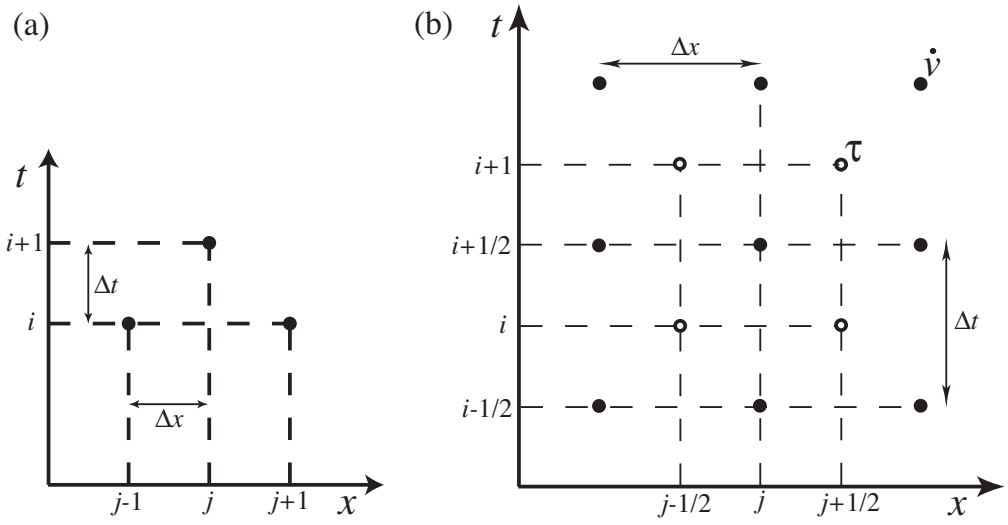

Figure 3.5: (a) A simple 1-D finite-difference gridding scheme. (b) A staggered grid in which the velocities and stresses are stored at different points.

To show how a centered finite-difference approach can be used to solve (3.54), consider Figure 3.5a, which shows the xt plane sampled at points $(i\Delta t, j\Delta x)$, where i and j are integers. We can then write

$$\begin{aligned} \frac{\dot{v}_j^{i+1} - \dot{v}_j^{i-1}}{2\Delta t} &= \frac{1}{\rho_j}\frac{\tau_{j+1}^i - \tau_{j-1}^i}{2\Delta x} \\ \frac{\tau_j^{i+1} - \tau_j^{i-1}}{2\Delta t} &= \mu_j \frac{\dot{v}_{j+1}^i - \dot{v}_{j-1}^i}{2\Delta x} \end{aligned} \tag{3.63}$$

This approach will be stable provided the time-mesh interval Δt is smaller than or equal to $\Delta x/c_j$, where $c_j = \sqrt{\mu_j/\rho_j}$ is the local wave velocity.

An even better algorithm uses a *staggered-grid* approach (e.g., Virieux, 1986) in which the velocities and stresses are computed at different grid points, offset by half a grid length in both x and t (see Figure 3.5b). In this case, we have

$$\begin{aligned} \frac{\dot{v}_j^{i+\frac{1}{2}} - \dot{v}_j^{i-\frac{1}{2}}}{\Delta t} &= \frac{1}{\rho_j}\frac{\tau_{j+\frac{1}{2}}^i - \tau_{j-\frac{1}{2}}^i}{\Delta x} \\ \frac{\tau_{j+1/2}^{i+1} - \tau_{j+1/2}^i}{\Delta t} &= \mu_{j+\frac{1}{2}} \frac{\dot{v}_{j+1}^{i+\frac{1}{2}} - \dot{v}_j^{i+\frac{1}{2}}}{\Delta x} \end{aligned} \tag{3.64}$$

As discussed in Aki and Richards (1980, p. 777), the error in this approximation is four times smaller than in (3.63) because the sampling interval has been halved.

Now let us consider the two-dimensional P-SV system. In this case $\mathbf{u} = (u, 0, w)$ and we can write:

$$\begin{aligned} \rho\frac{\partial^2 u}{\partial t^2} &= \partial_j \tau_{xj} = \frac{\partial \tau_{xx}}{\partial x} + \frac{\partial \tau_{xz}}{\partial z} \\ \rho\frac{\partial^2 w}{\partial t^2} &= \partial_j \tau_{zj} = \frac{\partial \tau_{zx}}{\partial x} + \frac{\partial \tau_{zz}}{\partial z} \end{aligned} \tag{3.65}$$

Using (3.50) we can obtain expressions for τ_{xx}, τ_{xz}, and τ_{zz}:

$$\begin{aligned} \tau_{xx} &= \lambda\left[\frac{\partial u}{\partial x} + \frac{\partial w}{\partial z}\right] + \mu\left[2\frac{\partial u}{\partial x}\right] \\ &= (\lambda + 2\mu)\frac{\partial u}{\partial x} + \lambda\frac{\partial w}{\partial z} \\ \tau_{xz} &= \mu\left[\frac{\partial u}{\partial z} + \frac{\partial w}{\partial x}\right] \\ \tau_{zz} &= \lambda\left[\frac{\partial u}{\partial x} + \frac{\partial w}{\partial z}\right] + \mu\left[2\frac{\partial w}{\partial z}\right] \\ &= (\lambda + 2\mu)\frac{\partial w}{\partial z} + \lambda\frac{\partial u}{\partial x} \end{aligned} \tag{3.66}$$

Equations (3.49) and (3.51) are a coupled system of equations for two-dimensional SH-wave propagation, while (3.65) and (3.66) are the equations for P-SV wave propagation. As in the one-dimensional case, it is often convenient to take time derivatives of the equations for the stress (3.51) and (3.66), so that we can express everything in terms of $(\dot{u}, \dot{v}, \dot{w}) = \frac{\partial \mathbf{u}}{\partial t}$. In this case the SH equations become:

$$\begin{aligned} \rho\frac{\partial \dot{v}}{\partial t} &= \frac{\partial \tau_{yx}}{\partial x} + \frac{\partial \tau_{yz}}{\partial z} \\ \frac{\partial \tau_{yx}}{\partial t} &= \mu\frac{\partial \dot{v}}{\partial x} \\ \frac{\partial \tau_{yz}}{\partial t} &= \mu\frac{\partial \dot{v}}{\partial z} \end{aligned} \tag{3.67}$$

and the P-SV equations become:

$$\begin{aligned} \rho\frac{\partial \dot{u}}{\partial t} &= \frac{\partial \tau_{xx}}{\partial x} + \frac{\partial \tau_{xz}}{\partial z} \\ \rho\frac{\partial \dot{w}}{\partial t} &= \frac{\partial \tau_{zx}}{\partial x} + \frac{\partial \tau_{zz}}{\partial z} \\ \frac{\partial \tau_{xx}}{\partial t} &= (\lambda + 2\mu)\frac{\partial \dot{u}}{\partial x} + \lambda\frac{\partial \dot{w}}{\partial z} \\ \frac{\partial \tau_{xz}}{\partial t} &= \mu\left[\frac{\partial \dot{u}}{\partial z} + \frac{\partial \dot{w}}{\partial x}\right] \\ \frac{\partial \tau_{zz}}{\partial t} &= (\lambda + 2\mu)\frac{\partial \dot{w}}{\partial z} + \lambda\frac{\partial \dot{u}}{\partial x} \end{aligned} \tag{3.68}$$

These are first-order systems of equations in velocity and stress which can be solved numerically. In this case, the elastic properties, ρ, λ, and μ are specified at a series of model grid points. With suitable starting conditions, the velocities and stresses are also defined at grid points. The program then calculates the required spatial derivatives of the stresses in order to compute the velocities at time $t + \Delta t$. The spatial derivatives of these velocites then allow the computation of new values for the stresses. This cycle is then repeated.

The global finite-difference calculation plotted in Figure 3.3 was performed using an axi-symmetric SH-wave algorithm developed and implemented by Igel and Weber (1995), Thorne et al. (2007) and Jahnke et al. (2008). It uses a staggered grid, with an eight-point operator to compute the spatial derivatives, and can be run on parallel computers with distributed memory.

3.10 EXERCISES

1. Period T is to angular frequency ω as wavelength Λ is to: (a) wavenumber k, (b) velocity c, (c) frequency f, (d) time t, (e) none of the above.

2. Figure 3.6 plots a harmonic plane wave at $t = 0$, traveling in the x direction at 5 km/s. (a) Write down an equation for this wave that describes displacement, u, as a function of x and t. (b) What is the maximum strain for this wave?

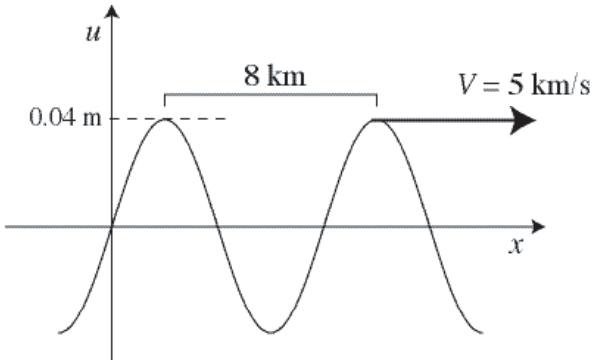

Figure 3.6: Displacement of a harmonic wave at $t = 0$ as a function of distance.

3. Consider two types of monochromatic plane waves propagating in the x direction in a uniform medium: (a) P-wave in which $u_x = A\sin(\omega t - kx)$, (b) S-wave with displacements in the y direction, i.e., $u_y = A\sin(\omega t - kx)$. For each case, derive expressions for the nonzero components of the stress tensor. Refer to (2.17) to get the components of the strain tensor; then use (2.30) to obtain the stress components.

4. Assume harmonic P-waves are traveling through a solid with $\alpha = 10$ km/s. If the maximum strain is 10^{-8}, what is the maximum particle displacement for waves with periods of: (a) 1 s, (b) 10 s, (c) 100 s?

5. Is it possible to have spherical symmetry for S-waves propagating away from a point source? Under what conditions could an explosive source generate shear waves?

6. Show that (3.46) satisfies (3.45) for $r \neq 0$.

7. (COMPUTER) In the case of plane-wave propagation in the x direction within a uniform medium, the homogeneous momentum equation (3.9) for shear waves can be expressed as

$$\frac{\partial^2 u}{\partial t^2} = \beta^2 \frac{\partial^2 u}{\partial x^2},$$

where u is the displacement. Write a computer program that uses finite differences to solve this equation for a bar 100 km in length, assuming $\beta = 4$ km/s. Use $dx = 1$ km for the length spacing and $dt = 0.1$ s for the time spacing. Assume a source–time function at $u(50 \text{ km})$ of the form

$$u_{50}(t) = \sin^2(\pi t/5), 0 < t < 5 \text{ s}.$$

Apply a stress-free boundary condition at $u(0 \text{ km})$ and a fixed boundary condition at $u(100 \text{ km})$. Approximate the second derivatives using the finite difference scheme:

$$\frac{\partial^2 u}{\partial x^2} = \frac{u_{i+1} - 2u_i + u_{i-1}}{dx^2}.$$

Plot $u(x)$ at 4 s intervals from 1 to 33 s. Verify that the pulses travel at velocities of 4 km/s. What happens to the reflected pulse at each end point? What happens when the pulses cross?

Hint: Here is the key part of a FORTRAN program to solve this problem:

```
(initialize t, dx, dt, tlen, beta and u1,u2,u3 arrays)
10    t=t+dt
      do i=2,100
         rhs=beta**2*(u2(i+1)-2.*u2(i)+u2(i-1))/dx**2
         u3(i)=dt**2*rhs+2.*u2(i)-u1(i)
      enddo
      u3(1)=u3(2)
      u3(101)=0.
      if (t.le.tlen) then
         u3(51)=sin(3.1415927*t/tlen)**2
      end if
      do i=1,101
         u1(i)=u2(i)
         u2(i)=u3(i)
      enddo
(output u2 at desired intervals, stop when t is big enough)
      go to 10
```